RESEARCH ON THE BEHAVIOR OF STEEL BEAM-TO-COLUMN CONNECTIONS

IN THE SEISMIC-RESISTANT STRUCTURE

Takeo Naka, Doctor of Eng. (I)
Ben Kato, Doctor of Eng. (II)
Makoto Watabe, Doctor of Eng. (III)
Masami Nakao, Master of Eng. (IV)

1. SYNOPSIS

This paper presents a summary of some research work done at the University of Tokyo on the behavior of beam-to-column connections for seismic-resistant structures. First, three elastic solutions of a column panel zone are proposed for assumed seismic forces. Then the results of such solutions are compared with experiments and good correlation is obtained in the elastic range. Beyond the elastic range which occurs at large loads, the response is idealized as bi-linear.

In the last part of the paper, general frame analysis is given with the necessary modifications introduced, because of the flexibility of the column panel zone. This flexibility is based on the theory presented above.

Nomenclature

A_{pc} (A_{pb})	:	Area of horizontal (vertical) cross-section in a panel zone.
V_p	:	Volume of a panel zone 4hbtp.
t_p	:	Thickness of a panel zone.
μ	:	Displacement of x direction.
v	:	Displacement of y direction.
σ_y	:	Yield strength of steel.
σ_B	:	Tensile strength of steel.
σ_q	:	Equivalent yield strength.
γ	:	Angular distortion of a panel zone.
τ_μ	:	Ultimate strength of a panel zone.
α_s	:	Stress concentration ratio ($A\sigma_{max}/P$).
A	:	Area.
P	:	Applied load.
σ_{max}	:	Maximum stress.
η	:	Connection efficiency factor ($P_B/\sigma_B A$).
P_B	:	Ultimate load.
$t_{b2(c2)}$	:	Thickness of beam (column) flange.
$B_{b(c)}$	:	Width of beam (column) flange.
$A_{effective}$	:	Effective area of A_{pc} for shear.

(I) Chairman and Professor of Engineering Dept., University of Tokyo.
(II) Associate Professor of Engineering Dept., University of Tokyo.
(III) Research Member of International Institute of Seismology and Earthquake Engineering, Building Research Institute, Research Fellow of Department of Civil Engineering, University of California.
(IV) Lecturer, Engineering Dept., University of Tokyo.

2. BEHAVIOR OF TYPICAL BEAM-TO-COLUMN CONNECTIONS IN FRAMES SUBJECTED TO LATERAL FORCE

2.1 FORCES AND DEFORMATIONS AT THE BOUNDARY OF A CONNECTION

2.1.a Derivation of Equations for Boundary Forces: Forces acting on the connection are assumed to act as shown in Fig. 2-1. Their positive sense and the symbols associated with these forces are as indicated. The isolated column web adjoining the beam and equal to the beam's depth will be referred to as the panel zone. It is convenient to define the load types acting on the panel zone as the "lateral load type" and the "vertical load type", as illustrated in Fig. 2-2.

$$M_{b1} = \frac{M_{b1} + M_{b2}}{2} + \frac{M_{b1} - M_{b2}}{2} = M_{ba} + M_{bd}$$

$$M_{b2} = \frac{M_{b1} + M_{b2}}{2} + \frac{M_{b1} - M_{b2}}{2} = M_{ba} - M_{bd}, \text{ etc.} \qquad 2\text{-}1$$

Any set of boundary forces on panel zone may be replaced by an equivalent system consisting at these forces. From equilibrium:

$$M_{ba} + M_{ca} + bQba + h\ Q_{ca} = 0$$

$$Q_{bd} + N_{ca} = 0,\ Q_{cd} + N_{ba} = 0 \qquad 2\text{-}2$$

The main problems relating to the "vertical load type" and to the "lateral load type" are illustrated in Fig. 2-3.

2.1.b Shear Forces Acting on Boundary of a Panel Zone: Forces T or C indicated in Fig. 2-4 can be expressed as

$$T \text{ or } C = \frac{M_{ba}}{2h} q_b \quad \text{and} \quad q_b = \frac{6t(\lambda + 1)}{(\lambda + 2t)^2 - \frac{1 - t/B_F}{\lambda + 2t} \lambda^3} \qquad 2\text{-}3$$

where q_b is the reduction ratio and subscripts b and c refer to beam and column, respectively.

In general, for wide flange section, the value of q_p is between 0.98 and 0.81. On this basis, the shear force acting on the boundary of a panel zone becomes

$$pQ_c = \frac{2M_{ba}}{2h} q_b + Q_{ca};\ pQ_b = \frac{2M_{ca}}{2b} q_c + Q_{ba} \qquad 2\text{-}4$$

2.1.c Normal Force Acting on the Boundary: Fig. 2-5 shows the state of stress acting on the panel zone. The value of these stresses caused by the normal forces on the boundaries are expressed by Eq. 2-5.

$$\pm\sigma_{M_{ba}} = \frac{3(1 - q_b) \cdot M_{ba}}{2h^2 \cdot t_p} \qquad \pm\sigma_{M_{ca}} = \frac{3(1 - q_c) \cdot M_{ca}}{2b^2 \cdot t_p}$$

$$\sigma_{N_{bd}} = \frac{N_{bd}}{A_B} \qquad \sigma_{N_{cd}} = \frac{N_{cd}}{A_c} \qquad 2\text{-}5$$

A_B : section area of beam
A_c : " " column

2.1.d Stresses in the Panel Zone:

i. Let q_b and q_c be 1.0 and assume that the shear stress is distributed uniformly over the section. Then the shear stress τ_p in a panel zone becomes

$$\tau_{p} = \frac{pQc}{A_{pc}} \text{ or } \frac{pQ_b}{A_{pb}} = \frac{M_{ba} + hQ_{ca}}{2b \cdot tp} = \frac{2M_{ba} + 2hQ_{ca}}{V_p} \text{ or } \frac{2M_{ca} + 2bQ_{ca}}{V_p} \qquad 2\text{-}6$$

This rather simple equation gives only approximate results.(V)

ii. Using the boundary stress conditions stated above, the stresses in the panel zone can be expressed by a stress function. For this purpose let stress function ϕ be

$$\phi = \frac{b_4}{3.2} x^3 y + \frac{d_4}{3.2} xy^3 + \frac{2}{a} x^2 + \frac{c_o}{2} y^2 - b_2 xy \qquad 2\text{-}7$$

whence the stresses become

$$\sigma_x = d_4 xy + c_2; \ \sigma_y = b_4 xy + a_2$$
$$\tau_{xy} = \frac{-d_4}{2} y^2 - \frac{b_4}{2} x^2 + b_2 \qquad 2\text{-}8$$

The coefficients a_2, b_2, c_2, b_4, and d_4 are determined from the boundary conditions and are as follows:

$$a_2 = \frac{N_{ca}}{A_c} \qquad C_2 = \frac{N_{ba}}{A_b}$$

$$b_2 = \frac{1}{V_p}\left\{(1-q_b) M_{ba} - (1-q_c) M_{ca} - 2(M_{ca} + b \cdot Q_{ba})\right\}$$

$$b_4 = \frac{-6(1-q_c)}{V_p \cdot b^2} M_{ca} \qquad d_4 = \frac{6(1-q_b)}{V_p \cdot h^2}$$

Deformations can be obtained by integration using the conditions:[1]

$$x = y = 0 \qquad \frac{\partial v}{\partial x} = \frac{\partial u}{\partial y}$$

$$u = \frac{1}{2E}\left[(d_4 - \nu b_4) X^2 Y + (c_2 - \nu a_2) \cdot 2X - \frac{1}{3}\left\{b_4 + (2+\nu) d_4\right\} Y^3 + 2(1+\nu) b_2 Y\right] \qquad 2\text{-}9$$

$$v = \frac{1}{2E}\left[(b_4 - \nu d_4) X Y^2 + (a_2 + \nu c_2) 2Y - \frac{1}{3}\left\{d_4 + (2+\nu) b_4\right\} X^3 + 2(1+\nu) b_2 X\right]$$

Theoretical shear stress distribution as given by Eq. 2-8 is illustrated in Fig. 2-6, where the vertical coordinate is taken as the value of shear stress. The highest shear stress occurs at the center of the panel zone. In this solution the stress caused by the vertical load type is assumed to be small and is neglected. It must be mentioned, however, that in case of external beam-to-column connections, this does not apply.

2.2 EXPERIMENTAL INVESTIGATIONS Five kinds of experiments have been performed, listed in Table 2-1. Some of the important results of these experiments are illustrated in Fig. 2-7 through Fig. 2-15. Specimens for experiment No. 1 were from a full-size model of a 17-story hotel structure. The column was of box-type with horizontal stiffeners penetrating the box section.

Specimens for experiment No. 2 had 5 different types of panel zones. Ten repeated reversed loads were applied to each specimen.

Experiment No. 3 was performed by S. Miki and his group.[3] The method of applying the load was not the same as that used in experiments

(V) A similar equation is recommended by L. S. Beedle, et al.[2]

No. 1 and 2. The specimens were about half the size.

The method of applying loads in experiment No. 4 was unique. Two specimens were tested to check the difference in behavior of the panel zone by changing the direction of the applied shear force, as indicated in Fig. 2-12.

For the purpose of checking the difference in behavior between the exterior beam-to-column connections and the interior ones, experiment No. 5 provided good information. The specimen was full size and 4 load reversals were applied.

2.3 BEHAVIOR OF PANEL ZONE

2.3.a Yield Strength: Three methods are proposed for estimating yield strength of panel zones. The first method is based upon Eq. 2-6; the second estimates yield strength from boundary conditions only. The third is based upon Eq. 2-8 using a stress function. The calculated yield strength by these three methods are indicated as c1, c2, and c3, respectively.

c1: Assuming yield strength for shear as $\sigma y/\sqrt{3}$ and using Eq. 2-6, we obtain the following equation:

$$\frac{\sigma y}{\sqrt{3}} = \frac{|2M_{ba} + 2hQ_{ca}|}{V_p} = \frac{|2M_{ca} + 2bQ_{ba}|}{V_p} \qquad 2\text{-}10$$

This equation gives a little higher than those found in experiments. With the exception of experiment No. 5, the results were from 10% to 30% lower than those given by Eq. 2-10.

c2: For the boundary conditions, as indicated in Fig. 2-5, the shear stress distribution may be calculated by the conventional beam theory. As before, Von Mises' criterion can be used for determining yield. This approach gives the yield strength which is in better agreement with the experimental results than that given by Eq. 2-10.

c3: As illustrated in Fig. 2-6, the maximum shear stress occurs in the center of the panel zone. The ratio of shear stress at the edge to the maximum at the center is between 1.0 and 2.0, depending upon the q and Q value in Eq. 2-8. Stresses at the center are:

$$\sigma_x = c_2 = \frac{N_{ba}}{A_B};\ \sigma_y = a_2 = \frac{N_{ca}}{A_c} \qquad 2\text{-}11$$

$$\tau_{xy} = b_2 = \frac{1}{V_p}\left[(1-q_b)\,M_{ba} - (1-q_c)\,M_{ca} - 2(M_{ca} + bd_{ba})\right]$$

On this basis the yield strength can be calculated from

$$\sigma_q = \sqrt{c_2^2 + a_2^2 - c_2\cdot a_2 + 3b_2^2} \qquad 2\text{-}12$$

It appears that the actual shear stress distribution in a panel zone is very close to the theoretical one, as illustrated in Fig. 2-6.

The photo-elastic experiment performed by Hisao Takahashi, et al.[4] is also available to corroborate this fact. Fig. 2-16 shows results of photo-elastic experiment on a beam-to-column connection. The contour line of the shear stress should theoretically become elliptical in shape, which can easily be seen from Fig. 2-6 or Eq. 2-8. Good agreement between the theoretical and experimental results suggests the proposed theoretical solution is adequate. It also must be mentioned, however, that the outer fringe of the photo-elastic picture tends to be of a rectangular shape instead of an elliptical one. Perhaps this is due to the disturbance of the stresses at a boundary which is neglected in the theoretical solution.

2.3.b Elastic Deformation: Three approaches, d1, d2, and d3, corresponding to the three methods c1, c2, and c3 are proposed. These three are indicated in figures.

d1: $\gamma = \tau/G \; : \; \gamma = d1 \qquad \tau = c1$ 2-13

Experimental results show that the value of d1 gives a very good approximation to the deformation of simple panel zone.

d2: In experiments No. 4 and No. 5, the effect of bending deformation must not be neglected to evaluate stiffness of the panel zone; therefore it is better to use the value d2, which includes shear deformation as well as bending deformation. In experiments No. 4 and No. 5, column flanges parallel to the web have some effective stiffness against shear force. The main idea of this theory is illustrated in Fig. 2-17. The results of experiment No. 4, in Fig. 2-13, support the above-mentioned idea, suggesting bi-linear relation between the apparent stress and strain.

d3: The deformation calculated by Eq. 2-9 is denoted d3 which corresponds to c3. Though c3 gives the exact value, value of d3 is not always the best among the three.

In order to confirm the validity of the boundary conditions, some analysis by stress function, using trigonometric series, was made. This study included a continuity condition of the column at a panel zone. Results are illustrated in Fig. 2-18, and the comparison of d1 and d3 is also made.

2.3.c Ultimate Strength and Plastic Deformation: It is recommended to estimate the ultimate strength of a panel zone by the following relation;

$$\tau_\mu = \frac{2M_{ba} + 2h\, Q_{ca}}{V_{p\ \text{effective}}} \leq \frac{\tau B}{\sqrt{3}}$$

This equation applies provided the panel zone does not buckle locally. The plastic deformation of the panel zone can be quite large. Based on experimental evidence, one can approximate the load-deflection of the panel zone by a by-linear relation.

2.4 FURTHER COMMENTS ON THE BEHAVIOR OF CONNECTIONS WITH THE "VERTICAL LOAD TYPE"(1,3,5)

The properties of the "lateral load type" are only possible when a beam flange and a column flange are welded to develop force T in Eq. 2-3. There must be a limiting relation between the flange width and their thicknesses in the beam-column assembly. Fig. 2-19 shows theoretical and experimental results. The solid line for $\eta = 1/\alpha$ indicates the elastic solution; the experimental results fall between the $2/\alpha$ and $2.5/\alpha$. This figure also suggests that the dimension of the column and the beam should be selected subject to the following limitation:

$$\frac{2}{3}\ \frac{t_{c2}^{3}}{t_{b2}\ B_{c}^{2}} = 0\ 009$$

By assuming $t_{c2}/Bc = 1/13$ and $B_c = B_b$, this equation reduces to the AISC's recommendation, "Specification for Design Fabrication and Election of Structural Steel for Building," 1963, to:

$$t_{c2} > 0.4\ \sqrt{B_b t_{b2}}$$

3. EXPERIMENTAL STUDY ON UNIQUE PANEL ZONE IN SHAPE

3.1. EXPERIMENTAL PROCEDURE

The dimensions of specimen and loading arrangements were selected in light of the results of Section 2. They are illustrated in Fig. 3-1. The main advantage of this kind of beam-to-column connection is that the beam flanges and the column flanges do not cross. Therefore, welding of the beam flanges to the column flanges in a perpendicular direction is eliminated. There is a total of five different types of plate-elements making up this kind of beam-to-column connection. A variety of thicknesses for plate elements were chosen resulting in 15 different kinds of specimens. Some of the results of this experimental program are illustrated in Fig. 3-2 and Fig. 3-5, in which the theoretical values calculated are also indicated. A theoretical approach to elastic shear stress distribution and to elastic deformation of a panel zone is based upon methods c2 and d2.

3.2 DISCUSSION OF EXPERIMENTAL RESULTS AND COMPARISON WITH THE PROPOSED THEORY

3.2.a Shear Stress Distribution: Good agreement between the experimental results and the theoretical prediction has been found (refer to Fig. 3-2 and Table 3-2). It must be noted that, among the 5 plates which make up the panel zone, the best agreement was achieved in the plate where the largest shear stress is found. This fact is indicated in Table 3-2.

3.2.b Deformation of the Connection: Fig. 3-2 illustrates the deformation property of one of the specimens. It can also be seen that the theoretical prediction was close to the experimental results. The ductility factors (μ) of the experimental results range between $\mu = 26.0$ (specimen No. 8) to $\mu - 57.0$ (specimen No. 15) as indicated in Table 3-1. The results also suggest that the deformation properties can be assumed as bi-linear.

3.2.c Strength of the Connection: The theoretical yield strength overestimates the real one by 5% to 23%. The ratio of the ultimate strength to the yield strength is between 2.2 and 2.52.

4. LATERAL FORCE FRAME ANALYSIS WITH THE INCLUSION OF THE SHEAR DISTRIBUTION AT CONNECTIONS

4.1. DISTORTION AND BOUNDARY FORCE RELATIONS In the analysis of frames which are subjected to earthquake motions, it is essential to know the hysteresis characteristics of frames. Fortunately, various kinds of hysteresis properties of panel zones or of frames as a whole are available from the results of many experiments[6,7]. A summary of these results, as well as $\tau_{mean} - \gamma$ properties in either elastic or plastic ranges are illustrated in Fig. 4-1. Stiffness of the panel zone in the plastic range is only 5% of the elastic. Hysteresis properties of a panel zone, in general, are quite stable as long as the members of the panel zone do not buckle. Distortion and boundary force relations are expressed in the revised form of Eq. 2-6 as

$$\frac{\gamma}{\alpha} \quad \frac{2M_{ba} + 2Q_{ca}}{G\,V_p} = \frac{M_{ca} + 2bQ_{ba}}{G\,V_p} \qquad 4\text{-}1$$

or as

$$\frac{\gamma}{\alpha} = \frac{M_{ba}}{G\,V_p} \qquad 4\text{-}2$$

4.2. <u>MODIFIED SLOPE DEFLECTION METHOD</u> The modified slope deflection method includes the shear deformations of beams, columns, and beam-to-column connections which are calculated by Eq. 4-1. The definition of terms and symbols are indicated in Fig. 4-2 and Eq. 4.3.

$$\left.\begin{array}{lll} RH1_k = -\dfrac{HD_{k,i}}{2\cdot H_k} & CA_{k,i} = CY_{k,i} + 0.5 & BA_{k,i} = BY_{k,i} + 0.5 \\ RH2_k = -\dfrac{HD_k}{2\cdot H_k} & CB_{k,i} = CY_{k,i} - 0.5 & BB_{k,i} = BY_{k,i} - 0.5 \\ RS1_{k,i} = -\dfrac{SD_{k,i}}{2\cdot S_{k,i}} & CC_{k,i} = 2\cdot CY_{k,i} & BC_{k,i} = 2\cdot BY_{k,i} \\ RS2_{k,i} = -\dfrac{SD_{k,i}}{2\cdot S_{k,i}} & CY_{k,i} = \dfrac{1.5}{1+\dfrac{2(1+\nu)\,K\cdot CK_{k,i}}{CAS_{k,i}\,H_k}} & BY_{k,i} = \dfrac{1.5}{1+\dfrac{2(1+\nu)\,K\cdot BK_{k,i}}{BAS_{k,i}\,S_{k,i}}} \end{array}\right\} \qquad 4\text{-}3$$

Then bending moments in the joint (k.i) are

$$\begin{bmatrix} \dfrac{M1_{k,i}}{CK_{k,i}} \\ \dfrac{M2_{k,i}}{BK_{k,i}} \\ \dfrac{M3_{k,i}}{CK_{k-1,i}} \\ \dfrac{M4_{k,i}}{BK_{k,i+1}} \end{bmatrix} = 2EK_0 \cdot \left[\begin{array}{ccccc|ccccc|cc} CA_{k,i}+CC_{k,i}\times RH2_k & CB_{k,i}+CC_{k,i}\times RH1_k & 0 & 0 & 0 & CC_{k,i}\times RH2_k & CC_{k,i}\times RH1_k & 0 & 0 & 0 & -CC_{k,i}\times(1+RH1_k+RH2_k) & 0 \\ \hline BA_{k,i}+BC_{k,i}\times RS2_{k,i} & 0 & BB_{k,i}+BC_{k,i}\times RS1_{k,i} & 0 & 0 & BA_{k,i} & 0 & BB_{k,i} & 0 & 0 & 0 & 0 \\ \hline CA_{k-1,i}+CC_{k-1,i}\times RH1_{k-1} & 0 & 0 & CB_{k-1,i}+CC_{k-1,i}\times RH2_{k-1} & 0 & CC_{k-1,i}\times RH1_{k-1} & 0 & 0 & CC_{k-1,i}\times RH2_{k-1} & 0 & 0 & -CC_{k-1,i}\times(1+RH1_{k-1}+RH2_{k-1}) \\ \hline BA_{k,i+1}+BC_{k,i+1}\times RS1_{k,i+1} & 0 & 0 & 0 & BB_{k,i+1}+BC_{k,i+1}\times RS2_{k,i+1} & BA_{k,i+1} & 0 & 0 & 0 & BB_{k,i+1} & 0 & 0 \end{array}\right] \begin{bmatrix} T_{k,i} \\ T_{k-1,i} \\ T_{k,i-1} \\ T_{k+1,i} \\ T_{k,i+1} \\ G_{k,i} \\ G_{k-1,i} \\ G_{k,i-1} \\ G_{k+1,i} \\ G_{k,i+1} \\ R_k \\ R_{k-1} \end{bmatrix} \qquad 4\text{-}4$$

By equilibrium of bending moment at the center of the panel zone (k-i),

$$-M1_{k,i} - M2_{k,i} - M3_{k,i} - M4_{k,i} - \frac{HD_k}{2}\cdot\left\{\frac{1}{H_k}\cdot(M1_{k,i} + M3_{k-1,i}) + \frac{1}{H_{k+1}}\cdot(M1_{k+1,i} + M3_{k,i})\right\}$$
$$-\frac{SD_{k,i}}{2}\cdot\left\{\frac{1}{S_{k,i}}\cdot(M2_{k,i} + M4_{k,i-1}) + \frac{1}{S_{k,i+1}}\cdot(M4_{k,i} + M2_{k,i+1})\right\} = 0 \qquad 4\text{-}5$$

Deformation of a panel zone as in Eq. 4-1 is represented in the following equation by using the notation of Eq. 4-3:

$$\frac{1}{\alpha_{k,i}}\cdot\frac{E}{2(1+\nu)}\cdot G_{k,i} = \frac{1}{TP_{k,i}\cdot HD_k}\left\{\frac{M1_{k,i}+M3_{k,i}}{SD_{k,i}} + \frac{M2_{k,i}+M4_{k,i-1}}{2\cdot S_{k,i}} + \frac{M4_{k,i}+M2_{k,i+1}}{2\cdot S_{k,i+1}}\right\} \qquad 4\text{-}6$$

By equilibrium of the external force and the internal reaction,

$$\frac{1}{H_k}\sum_i (M1_{k,i} + M3_{k-1,i}) = -\sum_k^r P_k \qquad 4\text{-}7$$

Substituting Eqs. 4-3 and 4-4 for Eqs. 4-5, and 4-7, Tables 4-1, 4-2, and 4-3 are obtained. This method is named the "micro-method" and is an "exact" solution. A model frame is illustrated in Fig. 4-3. The results of the micro-method of analysis, which neglects Q_{Ba} and Q_{Ca}, using Eq. 4-2, [8,9] and the conventional method, which includes shear deformation of columns and beams, and the ξ method,[10] which modifies the stiffness of columns and beams due to the shear distortion of a panel zone for the purpose of easy calculation, are all shown in Table 4-4 and Fig. 4-4.

5. CONCLUSIONS AND SUGGESTIONS FOR FUTURE STUDY

General concepts of the behavior of beam-to-column connections for lateral forces are well-established. However, further study of the behavior of various kinds of unique beam-to-column connections and the development of theoretical analysis for their plastic response appears to be desirable. An approach in such further studies using the "Finite Element Method" may be suitable. The results of this study indicate that if the panel zone is prevented from buckling, considerable energy absorption can be achieved, by developing a plastic mechanism in this zone. Fortunately, the undesirable P-Δ effect appears to be small[11] and hence plastic deformation at the panel zone may be tolerated.

Bibliography

1. Naka, T., et al., "Research on the behavior of the beam-to-column connections," Laboratory for steel structure, U. of Tokyo, 1967.
2. Beedle, L. S., et al., "Plastic design of multi-story frames," Lecture notes, Vol. 1, Lehigh University, 1965.
3. Miki, S., et al., "Experimental study of steel connections," Seminar of Kanto district, Architecture Institute of Japan, May 1964.
4. Takahashi, J., "Photo-elastic experiment on the connection," Report from Ohbayashi Gumi Company, 1965.
5. Ohmori, N., et al., "Load Test of Beam Column Connection of Steel Frame for Kasumigaseki Mitsui," Research report from Kajima Institute of Construction Technology, 1964.
6. Popov, E. P., et al., "Behavior of steel building connections subjected to repeated inelastic strain," SESM Report No. 67-30, U. of California, Berkeley, 1967.
7. Igarashi, S., "Experimental study on the hysteretic characteristics and damping capacity of steel connections," Transactions of the Architectural Institute of Japan, No. 75, August 1963.
8. Muto, K., "Method of Frame Analysis in Consideration of Pure Shear Panel Deformation," Report from Muto Laboratory, 1967.
9. Tanaka, H., "Slope deflection method for frames with connections having a web deformed by shear force," Transactions of the Architectural Institute of Japan, No. 109, March 1965.
10. Takeda, H., "An approximation method of stress analysis of multi-story frame subjected to horizontal force, including consideration of shear deformation of beam-to-column-connective zone," Transactions of the Architectural Institute of Japan, No. 108, February 1965.
11. Goel, S. C., "The response of steel frame structures to earthquake forces," Part II, AISI Project No. 119, December 1967.

Acknowledgments

We would like to express our appreciation for the help given by Prof. E. P. Popov, of the U. of California. Our gratitute is also expressed to Elizabeth Jaynes and Carmella Bryant, for help in editing and typing.

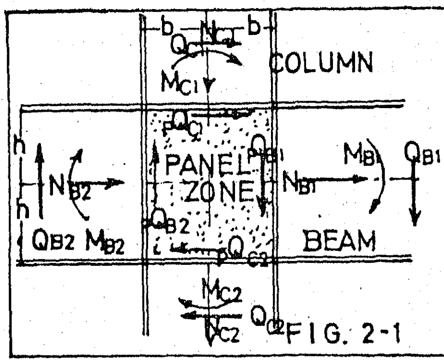

FIG. 2-1

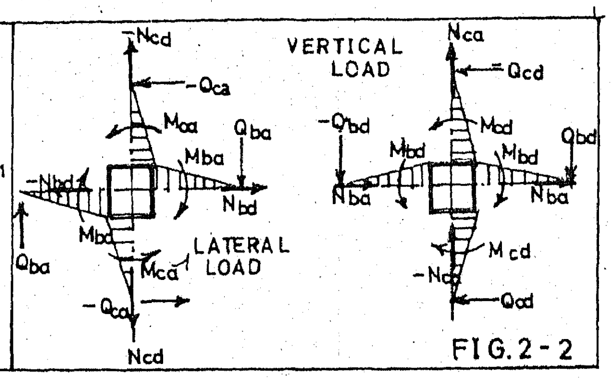

FIG. 2-2

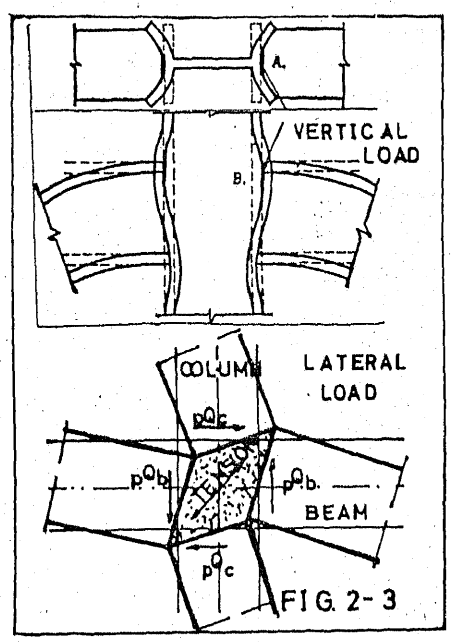

FIG. 2-3

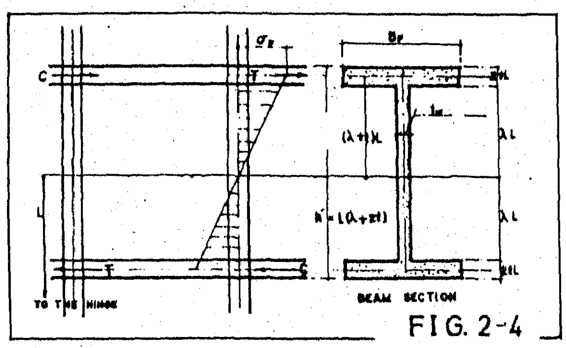

FIG. 2-4

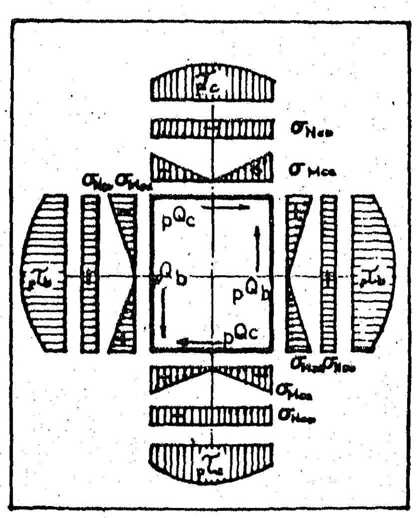

STRESSES AROUND THE PANEL ZONE FIG. 2-5

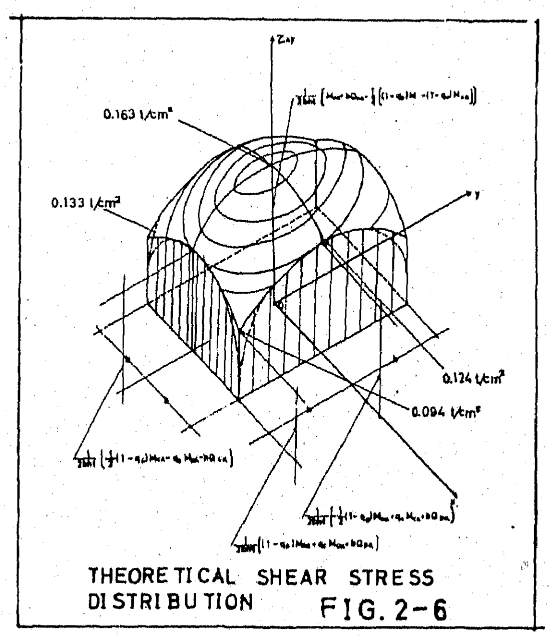

THEORETICAL SHEAR STRESS DISTRIBUTION FIG. 2-6

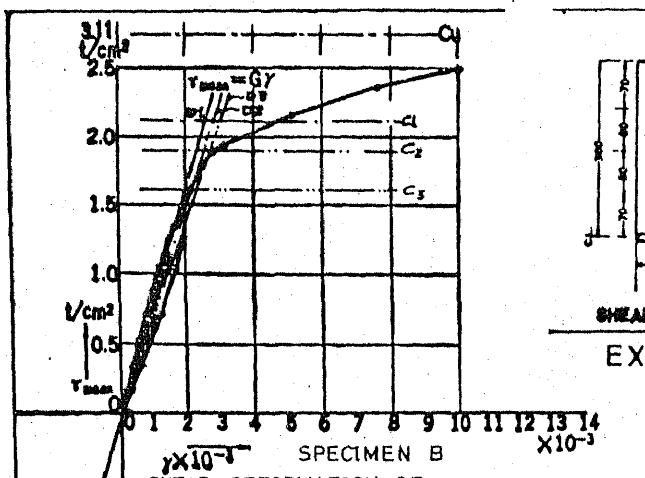

SHEAR DEFORMATION OF PANEL ZONE
EXP. NO1 FIG. 2-7

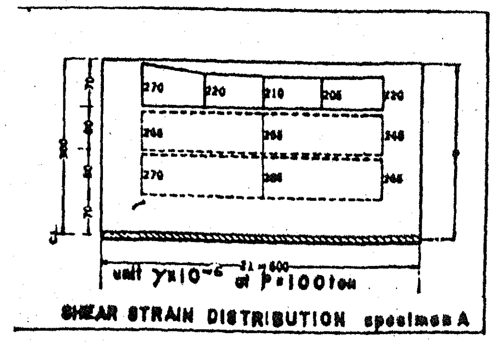

EXP. NO1 FIG. 2-8

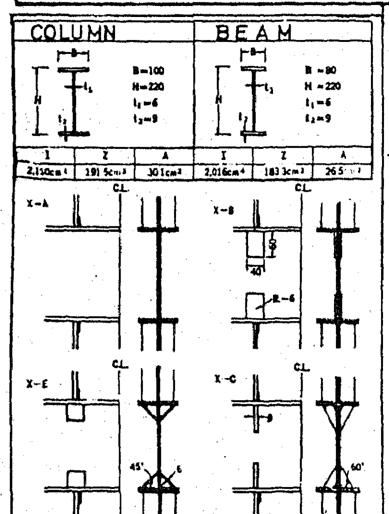

EXP. NO2
VARIETY OF SPECIMEN
FIG. 2-9

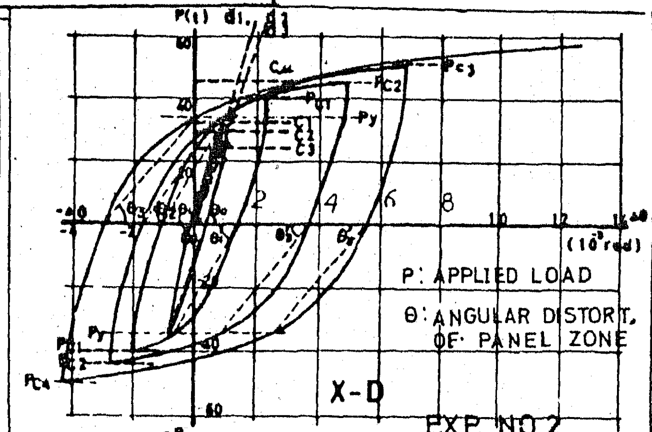

EXP. NO2

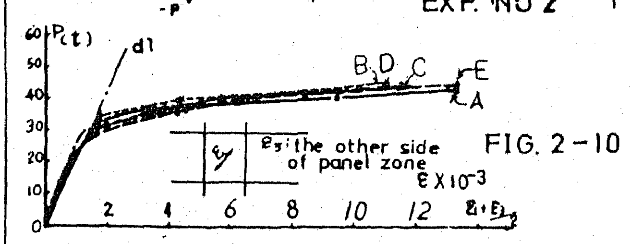

FIG. 2-10

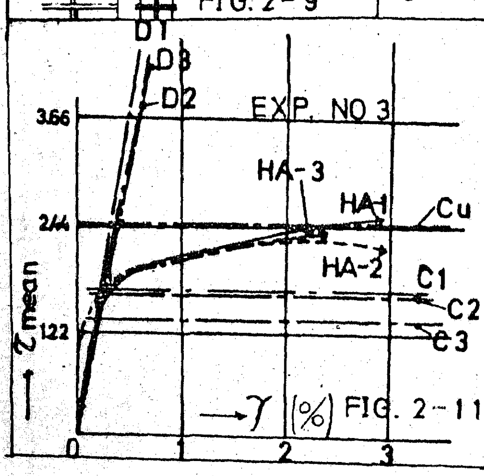

FIG. 2-11

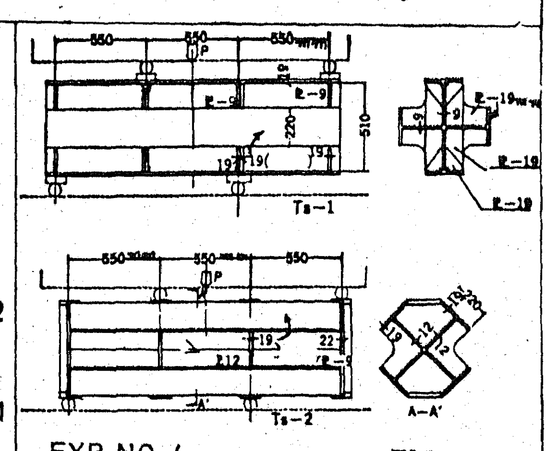

EXP. NO 4 FIG 2-12

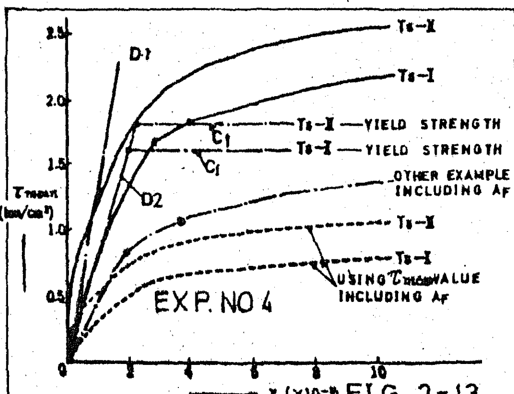

FIG. 2-13

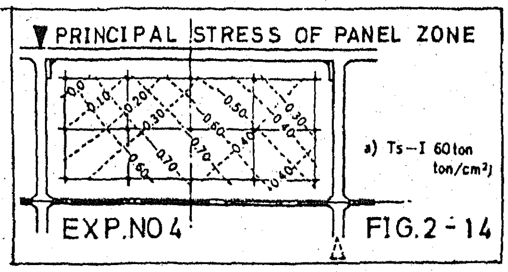

FIG. 2-14

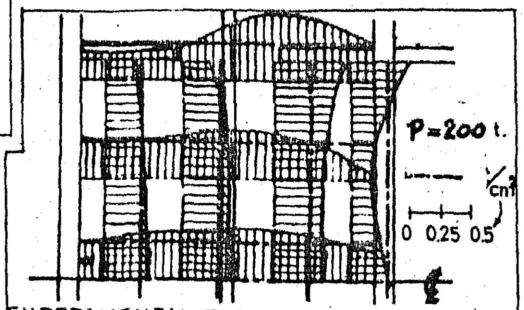

EXPERIMENTAL RESULTS OF SHEAR STRESS DISTRIBUTION IN PANEL ZONE

EXP.NO.5 FIG. 2-15

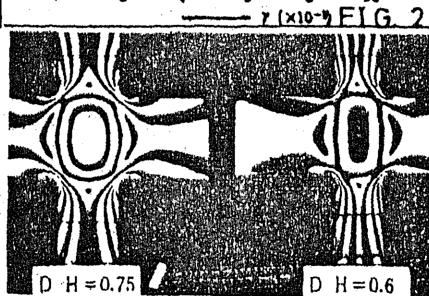

EXAMPLE of PHOTELASTIC TEST

FIG. 2-16

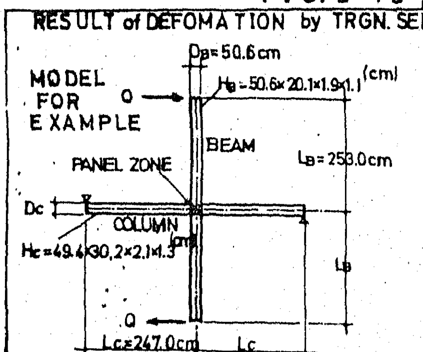

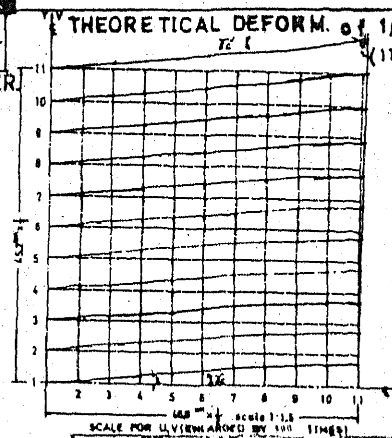

		d1	d3	TRIG SER.
		×10⁻³ Rad/ton	×10⁻³ Rad/ton	×10⁻³ Rad/ton
γ_c'		0.209	0.210	0.247
	U		cm 0.205	cm 0.63C
11,11	V		cm 4.670	cm 5.150

$\gamma c = 0.139 \times 10^{-3}$ cm

FIG. 2-18

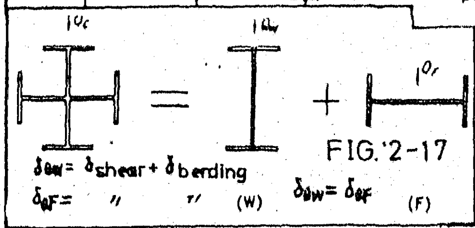

FIG. 2-17

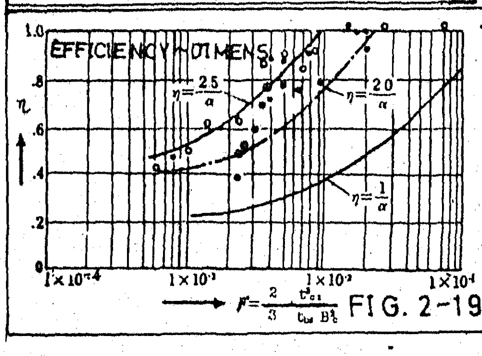

FIG. 2-19

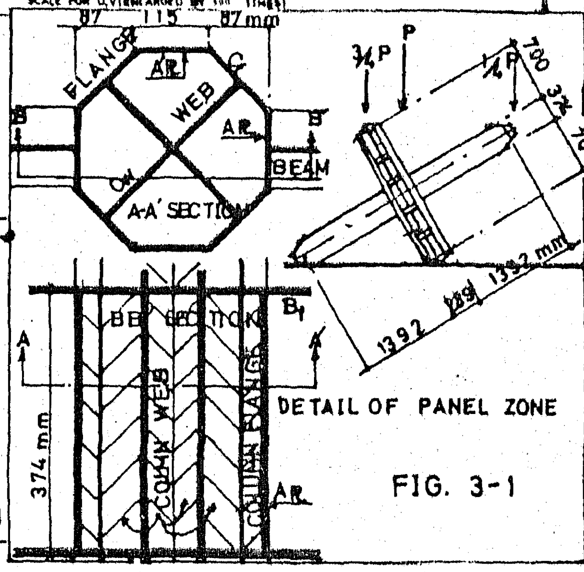

FIG. 3-1

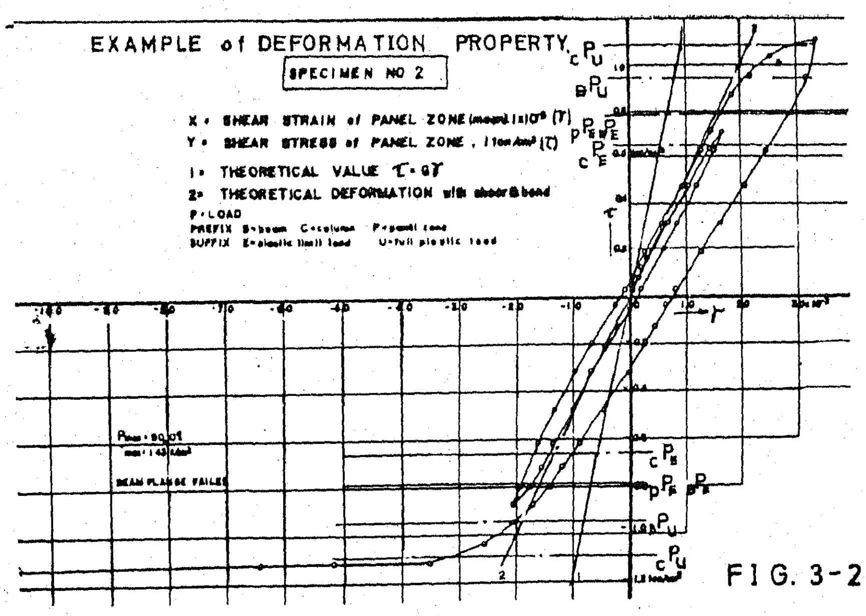

FIG. 3-2

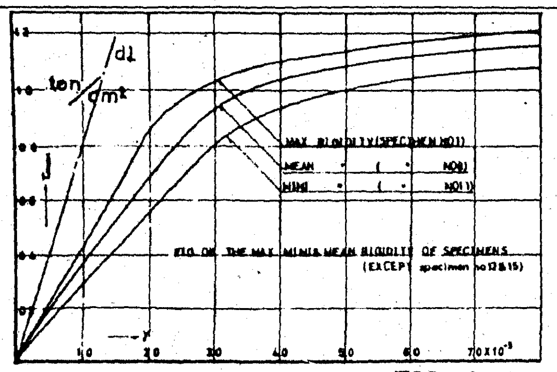

FIG. 3-3

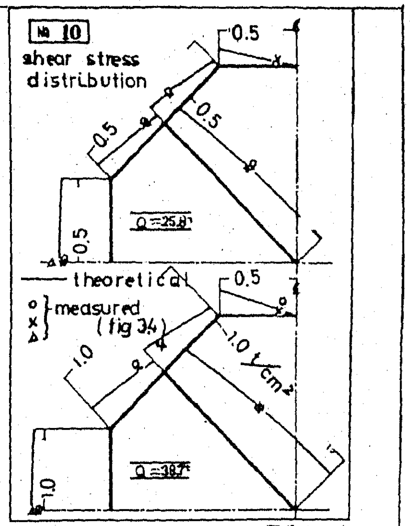

FIG. 3-5

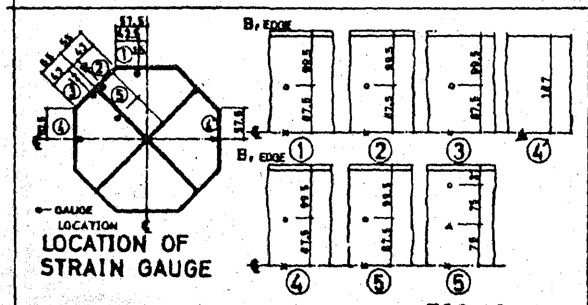

FIG. 3-4

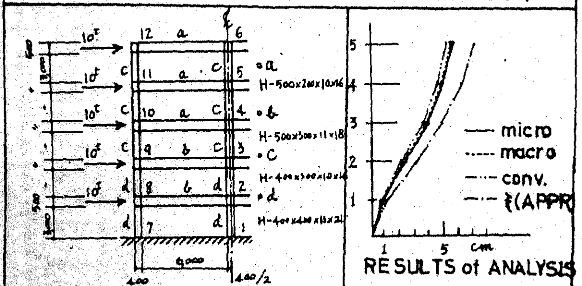

MODEL STRCTURE FIG. 4-3

RESULTS of ANALYSIS

FIG. 4-4

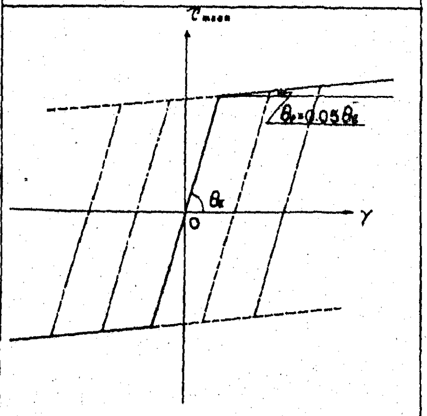

SIMPLIFIED HYSTERETIC PROPERTY OF GENERAL PANEL ZONE

FIG. 4-1

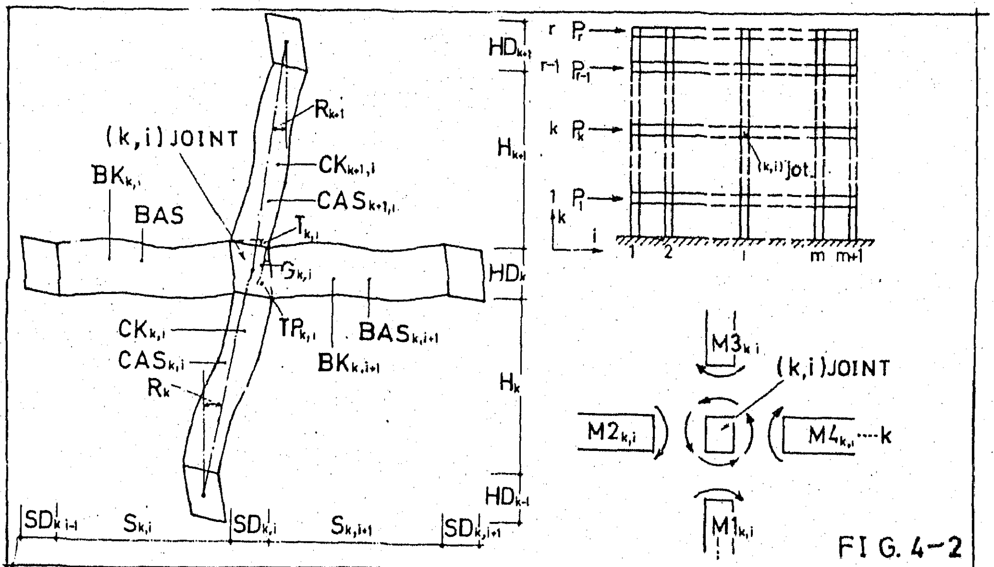

FIG. 4-2

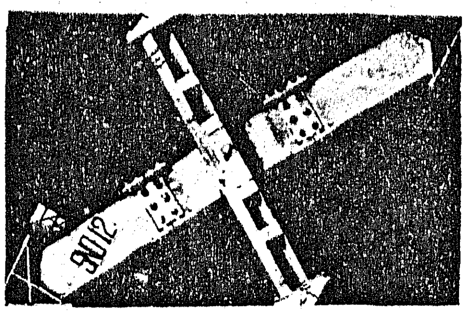

SPECIMEN TESTED PH. 3-1

TABLE 2-2

specimen no	yield τ strength	ultimate strength	maximum ductility factor	place failed
X-A	1.47 t/cm²	2.18 t/cm²	31.0	PANEL ZONE BUCKLED
X-B	1.82 t/cm²	2.98 "	30.0	"
X-C	1.52 "	2.80 "	19.7	"
X-D	1.72 "	3.13 "	27.1	"
X-E	1.52 "	2.70 "	12.8	"

THRETICAL DEFORMATION& STRENGTH

1	τ_{max} = 1.63 t/cm² γ = 1.[illegible] ×10⁻³	2	τ_{max} = 1.82 γ = 1.43	3	τ_{max} = 1.24 γ = 1.48

TEST RESULTS of ALL SPECIMEN

TABLE 3-1

μ. THE MAXIMUM DUCTILITY FACTOR
τY. value yielded γY. value yielded

No.	BEHAVIOR OF SPECIMEN	THE PLACE FAILED	τ_{max} t/cm²	γ_{max} ×10	τY t/cm²	τY/γY t/cm²×10
1	beam flanges started to be buckled at τ_{max}=1.17t/cm² and welding part around A'R was dislocated.	beam flange was buckled.	1.43	14.Γ	0.85	0.455
2	shear deformation of A'R was quite conspicuous	beam web was buckled	1.43	16.2	0.87	0.424
3	shear deformation of A'R was conspicuous beam flange was buckled subsequently beam web was also buckled	beam web was buckled	1.46	28.7	(.70	0.500
4	beam flange was buckled subsequently beam web was also buckled shear deformation was not so conspicuous	beam web was buckled	1 05	..8	0.59	0.416
5	beam flange was buckled subsequently column flange and beam web were buckled simultaneously	column flange was buckled	1.32	14.5	0.83	0.424
c	shear deformation of A'R was quite conspicuous and welding boundary around A'R was dislocated	welding boundary of A'R was torn off then A'R was buckled μ=28.6	1.50	32.0	0.73	0.403
-	beam flange and web started to be buckled at τ_{max}=1.39t/cm²	beam web was buckled	1.53	34.4	0.70	0.526
8	shear deformation of A'R was quite conspicuous and finally began to be torn off	welding boundary of A'R was torn off at two directions then A'R was buckled μ=26.0	1 77	67.3	0.67	0.425
0	at the edge of beam flange deformation was remarkable	beam flange was broken off at the end	0.75	3.5	0.45	0.315
10	deformation of A'R was quite conspicuous and the component of bending deformation of A'R was also witnessed	beam web was buckled μ=29.4	1 53	43.5	0.63	0.416
11	beam flange and web started to be buckled	beam web was buckled	1.24	15.2	0.73	0.286
12	Quite same behavior of specimen No.9	beam flange was broken off	0.61	3.0	0.45	0.266
13	deformation of panel zone as a whole was remarkable and welding boundary around A'R was dislocated	beam flange and web were torn μ=29.0	1.55	54.6	0.75	0.400
14	Quite same behavior of specimen No.13	beam flange and web were torn off μ=40.0	1.54	63.1	0.56	0.357
15	shear deformation of panel zone as a whole was conspicuous and column web in panel zone began to be buckled	column web in panel zone was buckled μ=57.0	1.46	80.1	0.40	0.286

TABLE 2-1

THE LIST OF EXPERIMENT

NUMBER	COLUMN SECTION TYPE	COLUMN DIMENSION mm	BEAM SECTION TYPE	BEAM DIMENSION mm	LOADING TYPE	NUMBER of SPECIMEN	LABORATORY
1	box type	a×b×t 600×600×28 FULL SCALE	H	494 x 300x12 x 22mm		1 θ=45° 1 θ=17.5°	NAKA, KATO LAB.
2	H	220×100×6×9 MODEL	H (a×b×t_1×t_2)	a x b x t_1 x t_2 220x80x 6 x 9		5 VARIATION of stiffener	〃
3	H	200×100×8×12 MODEL	H	200 x 100 x 5.6 x 8.5		3 variation of loading cycle	S.MIKI KAWASAKI HEAVY IND. RESEARCH LAB.
4		546×220×9×19 ×2 (double) FULL SCALE	no beam was attached	BEAM DEPTH WAS ASSUMED TO be 550mm		2 vari. loading direction	NAKA, KATO LAB.
5		680×350×25×30 ×2 FULL SCALE	H	950 x 300 x 16 x 32			〃

TABLE 4-1

V.	C.
$T_{k,i}$	$0.5 \cdot CK_{k,i} \cdot \{1+(1+2 \cdot RH2_k)^2 \cdot CC_{k,i}\} + 0.5 \cdot CK_{k+1,i} \cdot \{1+(1+2 \cdot RH1_{k+1})^2 \cdot CC_{k+1,i}\}$ $+0.5 \cdot BK_{k,i} \cdot \{1+(1+2 \cdot RS2_{k,i})^2 \cdot BC_{k,i}\} + 0.5 \cdot BK_{k,i+1} \cdot \{1+(1+2 \cdot RS1_{k,i+1})^2 \cdot BC_{k,i+1}\}$
$T_{k-1,i}$	$0.5 \cdot CK_{k,i} \cdot \{(1+2 \cdot RH2_k)(1+2 \cdot RH1_k) CC_{k,i} - 1\}$
$T_{k,i-1}$	$0.5 \cdot BK_{k,i} \cdot \{(1+2 \cdot RS2_{k,i})(1+2 \cdot RS1_{k,i}) \cdot BC_{k,i} - 1\}$
$T_{k+1,i}$	$0.5 \cdot CK_{k+1,i} \cdot \{(1+2 \cdot RH1_{k+1})(1+2 \cdot RH2_{k+1}) \cdot CC_{k+1,i} - 1\}$
$T_{k,i+1}$	$0.5 \cdot BK_{k,i+1} \cdot \{(1+2 \cdot RS1_{k,i+1})(1+2 \cdot RS2_{k,i+1}) \cdot BC_{k,i+1} - 1\}$
$G_{k,i}$	$CK_{k,i} \cdot (1+2 \cdot RH2_k) \cdot RH2_k \cdot CC_{k,i} + CK_{k+1,i} \cdot (1+2 \cdot RH1_{k+1}) \cdot RH1_{k+1} \cdot CC_{k+1,i}$ $+0.5 \cdot BK_{k,i} \cdot \{(1+2 \cdot RS2_{k,i}) \cdot BC_{k,i} + 1\} + 0.5 \cdot BK_{k,i+1} \cdot \{(1+2 \cdot RS1_{k,i+1}) \cdot BC_{k,i+1} + 1\}$
$G_{k-1,i}$	$CK_{k,i} \cdot (1+2 \cdot RH2_k) \cdot RH1_k \cdot CC_{k,i}$
$G_{k,i-1}$	$0.5 \cdot BK_{k,i} \cdot \{(1+2 \cdot RS2_{k,i}) \cdot BC_{k,i} - 1\}$
$G_{k+1,i}$	$CK_{k+1,i} \cdot (1+2 \cdot RH1_{k+1}) \cdot RH2_{k+1} \cdot CC_{k+1,i}$
$G_{k,i+1}$	$0.5 \cdot BK_{k,i+1} \cdot \{(1+2 \cdot RS1_{k,i+1}) \cdot BC_{k,i+1} - 1\}$
R_k	$-CK_{k,i} \cdot (1+2 \cdot RH2_k)(1+RH1_k+RH2_k) \cdot CC_{k,i}$
R_{k+1}	$-CK_{k+1,i} \cdot (1+2 \cdot RH1_{k+1})(1+RH1_{k+1}+RH2_{k+1}) \cdot CC_{k+1,i}$

moment equil. $\Sigma(V.) \times (C.) = 0$ ----------

TABLE 4-2

V.	C.
$T_{k,i}$	$0.5 \cdot CK_{k,i} \cdot \{(1+2 \cdot RH2_k) \cdot CC_{k,i} + 1\} + 0.5 \cdot CK_{k+1,i} \cdot \{(1+2 \cdot RH1_{k+1}) \cdot CC_{k+1,i} + 1\}$ $+BK_{k,i} \cdot (1+2 \cdot RS2_{k,i}) \cdot RS2_{k,i} \cdot BC_{k,i} + BK_{k,i+1} \cdot (1+2 \cdot RS1_{k,i+1}) \cdot RS1_{k,i+1} \cdot BC_{k,i+1}$
$T_{k-1,i}$	$0.5 \cdot CK_{k,i} \cdot \{(1+2 \cdot RH1_k) \cdot CC_{k,i} - 1\}$
$T_{k,i-1}$	$BK_{k,i} \cdot (1+2 \cdot RS1_{k,i}) \cdot RS2_{k,i} \cdot BC_{k,i}$
$T_{k+1,i}$	$0.5 \cdot CK_{k+1,i} \cdot \{(1+2 \cdot RH2_{k+1}) \cdot CC_{k+1,i} - 1\}$
$T_{k,i+1}$	$BK_{k,i+1} \cdot (1+2 \cdot RS2_{k,i+1}) \cdot RS1_{k,i+1} \cdot BC_{k,i+1}$
$G_{k,i}$	$CK_{k,i} \cdot RH2_k \cdot CC_{k,i} + CK_{k+1,i} \cdot RH1_{k+1} \cdot CC_{k+1,i}$ $+BK_{k,i} \cdot RS2_{k,i} \cdot BC_{k,i} + BK_{k,i+1} \cdot RS1_{k,i+1} \cdot BC_{k,i+1} - \frac{1}{\alpha_{k,i}} \cdot \frac{TP_{k,i} \cdot HD_k \cdot SD_{k,i}}{4 \cdot (1+\nu) \cdot K_0}$
$G_{k-1,i}$	$CK_{k,i} \cdot RH1_k \cdot CC_{k,i}$
$G_{k,i-1}$	$BK_{k,i} \cdot RS2_{k,i} \cdot BC_{k,i}$
$G_{k+1,i}$	$CK_{k+1,i} \cdot RH2_{k+1} \cdot CC_{k+1,i}$
$G_{k,i+1}$	$BK_{k,i+1} \cdot RS1_{k,i+1} \cdot BC_{k,i+1}$
R_k	$-CK_{k,i} \cdot (1+RH1_k+RH2_k) \cdot CC_{k,i}$
R_{k+1}	$-CK_{k+1,i} \cdot (1+RH1_{k+1}+RH2_{k+1}) \cdot CC_{k+1,i}$

deformation of panel zone $\Sigma(V.) \times (C.) = 0$ ----------

TABLE 4-3

V.	C.
$T_{k,i}$	$CK_{k,i} \cdot (1+2 \cdot RH2_k) \cdot CC_{k,i}$
$T_{k-1,i}$	$CK_{k,i} \cdot (1+2 \cdot RH2_k) \cdot CC_{k,i}$
$G_{k,i}$	$2 \cdot CK_{k,i} \cdot RH2_k \cdot CC_{k,i}$
$G_{k-1,i}$	$2 \cdot CK_{k,i} \cdot RH1_k \cdot CC_{k,i}$
R_k	$-2 \cdot (1+RH1_k+RH2_k) \cdot \sum_i CK_{k,i} \cdot CC_{k,i}$

equil. of ex. & int. forces $\Sigma(V.) \times (C.) = -\frac{H_k}{2EK_0} \sum_k^{f} P_k$ -----

TABLE 3-2

POINT NO	mean	σ_s
1	97.6 %	32.1 %
2	74.4	9.6
3	89.1	10.4
4	94.2	12.1
5	99.5	9.2

mean: mean ratio of results to theoretical value

σ_s : standard deviation

TABLE 4-4

results of moments.

NO.		mic.	mac.	conv.	ζ
6	M1	-10.4	0.982	0.905	0.957
	M2, M4	5.4	0.944	0.917	0.967
5	M1	-16.2	0.987	0.787	0.991
	M2, M4	11.3	[illegible]	[illegible]	[illegible]
	M3	4.5	1.001	1.280	1.220
4	M1	-20.2	0.983	1.006	1.013
	M2, M4	17.0	0.896	1.058	1.053
	M3	-10.8	0.985	1.150	1.120
3	M1	-26.3	0.972	1.077	1.030
	M2, M4	24.8	0.895	1.069	1.069
	M3	-19.1	0.983	1.065	1.086
2	M1	-14.2	0.994	1.300	1.217
	M2, M4	24.0	0.867	1.077	1.042
	M3	-28.0	0.978	0.974	0.995
1		-42.7	0.982	0.962	0.900
		moment ton-m	ratio to micro method		